4934 *Chem. Mater.* **2009,** *21,* 4934–4939
DOI:10.1021/cm902102k

CHEMISTRY OF MATERIALS
Article

# Electrochemical Reduction of Silver Vanadium Phosphorus Oxide, $Ag_2VO_2PO_4$: The Formation of Electrically Conductive Metallic Silver Nanoparticles

Esther S. Takeuchi,*[,†,‡,§] Amy C. Marschilok,[‡] Kevin Tanzil,[†] Eric S. Kozarsky,[‡] Shali Zhu,[§] and Kenneth J. Takeuchi*[,§]

[†]*Department of Chemical and Biological Engineering and* [‡]*Department of Electrical Engineering and* [§]*Department of Chemistry, University at Buffalo* (*SUNY*)*, Buffalo, New York 14260*

*Received July 11, 2009. Revised Manuscript Received August 26, 2009*

As a cathode material, silver vanadium phosphorus oxide ($Ag_2VO_2PO_4$) displays several notable electrochemical properties: large capacity, high current capability, and an effective delivery of high current pulses. These cell performance characteristics can be attributed to the presence of silver nanoparticles formed in situ during the electrochemical reduction of $Ag_2VO_2PO_4$. Specifically, changes in the composition and structure of $Ag_2VO_2PO_4$ with reduction, especially the formation of silver nanoparticles, are detailed to rationalize a 15 000 fold increase in conductivity with initial discharge, which can be related to the power characteristics associated with $Ag_2VO_2PO_4$ cathodes in primary lithium batteries.

## Introduction

Polyanion compounds in the general class of $MPO_4$ are receiving significant attention in journal publications as materials for energy storage applications, most generally with compositions such as $Li_xMPO_4$, where M equals Fe, Mn, or VO.[1−9] The materials demonstrate exceptional stability and can provide high voltage and capacity when used in lithium based batteries, but their characteristically low electrical conductivities[10−14] are their biggest challenge for implementation as battery materials. To enhance $Li_xMPO_4$ electrical conductivity, several strategies have emerged in the scientific literature, including coating of $Li_xMPO_4$ particles with carbon,[15,16] cosynthesizing the $Li_xMPO_4$ materials with carbon to achieve intimate contact of the particles with the conductive material,[13,17] adding silver and copper powder to the $Li_xMPO_4$ matrix to achieve improved conductivity,[18,19] or the solid-solution doping of $LiFePO_4$.[20] Unfortunately, the strategies involving the addition of an external conducting material require additional processing steps and can significantly reduce energy density because of the presence of the extraneous inert conducting material.

Another family of materials, copper vanadium oxides, has also been the subject of a number of recent published studies as cathode materials for primary and rechargeable systems.[21−29] Notably, the electrochemical reduction of copper vanadium oxide occurs with the formation of very

*Corresponding author. E-mail: et23@buffalo.edu (E.T.); takeuchi@buffalo.edu (K.T.). Phone: (716) 645-1185 (E.T.); (716) 645-1494 (K.T.). Fax: (716) 645-3822 (E.T.); (716) 645-6963 (K.T.).

(1) Yang, H.; Wu, X.-L.; Cao, M.-H.; Guo, Y.-G. *J. Phys. Chem. C* **2009**, *113*(8), 3345–3351.
(2) Chang, C.; Xiang, J.; Shi, X.; Han, X.; Yuan, L.; Sun, J. *Electrochim. Acta* **2008**, *54*(2), 623–627.
(3) Delmas, C.; Maccario, M.; Croguennec, L.; Le Cras, F.; Weill, F. *Nat. Mater.* **2008**, *7*(8), 665–671.
(4) Zhou, X.; Liu, Y.; Guo, Y. *Solid State Commun.* **2008**, *146*(5−6), 261–264.
(5) Li, Z.; Zhang, D.; Yang, F. *J. Mater. Sci.* **2009**, *44*(10), 2435–2443.
(6) Liao, X.-Z.; Ma, Z.-F.; He, Y.-S.; Zhang, X.-M.; Wang, L.; Jiang, Y. *J. Electrochem. Soc.* **2005**, *152*(10), A1969–A1973.
(7) Song, Y.; Zavalij, P. Y.; Whittingham, M. S. *J. Electrochem. Soc.* **2005**, *152*(4), A721–A728.
(8) Franger, S.; Bourbon, C.; Le Cras, F. *J. Electrochem. Soc.* **2004**, *151*(7), A1024–A1027.
(9) Martha, S. K.; Markovsky, B.; Grinblat, J.; Gofer, Y.; Haik, O.; Zinigrad, E.; Aurbach, D.; Drezen, T.; Wang, D.; Deghenghi, G.; Exnar, I. *J. Electrochem. Soc.* **2009**, *156*(7), A541–A552.
(10) Tarascon, J. M.; Armand, M. *Nature* **2001**, *414*(6861), 359–67.
(11) Gaubicher, J.; Mercier, T. L.; Chabre, Y.; Angenault, J.; Quarton, M. *J. Electrochem. Soc.* **1999**, *146*(12), 4375–4379.
(12) Amine, K.; Yasuda, H.; Yamachi, M. *Electrochem. Solid-State Lett.* **2000**, *3*(4), 178–179.
(13) Huang, H.; Yin, S. C.; Nazar, L. F. *Electrochem. Solid-State Lett.* **2001**, *4*(10), A170–A172.
(14) Yang, S.; Song, Y.; Zavalij, P. Y.; Stanley Whittingham, M. *Electrochem. Commun.* **2002**, *4*(3), 239–244.
(15) Herstedt, M.; Stjerndahl, M.; Nyten, A.; Gustafsson, T.; Rensmo, H.; Siegbahn, H.; Ravet, N.; Armand, M.; Thomas, J. O.; Edstrom, K. *Electrochem. Solid-State Lett.* **2003**, *6*(9), A202–A206.
(16) Ravet, N.; Chouinard, Y.; Magnan, J. F.; Besner, S.; Gauthier, M.; Armand, M. *J. Power Sources* **2001**, *97−98*, 503–507.
(17) Prosini, P. P.; Zane, D.; Pasquali, M. *Electrochim. Acta* **2001**, *46* (23), 3517–3523.
(18) Park, K. S.; Son, J. T.; Chung, H. T.; Kim, S. J.; Lee, C. H.; Kang, K. T.; Kim, H. G. *Solid State Commun.* **2004**, *129*(5), 311–314.
(19) Croce, F.; D'Epifanio, A.; Hassoun, J.; Deptula, A.; Olczac, T.; Scrosati, B. *Electrochem. Solid-State Lett.* **2002**, *5*(3), A47–A50.
(20) Chung, S.-Y.; Bloking Jason, T.; Chiang, Y.-M. *Nat. Mater.* **2002**, *1*(2), 123–8.
(21) Ma, H.; Zhang, S.; Ji, W.; Tao, Z.; Chen, J. *J. Am. Chem. Soc.* **2008**, *130*(15), 5361–5367.
(22) Tarascon, J. M.; Delacourt, C.; Prakash, A. S.; Morcrette, M.; Hegde, M. S.; Wurm, C.; Masquelier, C. *Dalton Trans.* **2004**, No. 19, 2988–2994.
(23) Garcia-Alvarado, F.; Tarascon, J. M. *Solid State Ionics* **1993**, *63−65*(1−4), 401–6.
(24) Garcia-Alvarado, F.; Tarascon, J. M.; Wilkens, B. *J. Electrochem. Soc.* **1992**, *139*(11), 3206–14.
(25) Coustier, F.; Jarero, G.; Passerini, S.; Smyrl, W. H. *J. Power Sources* **1999**, *83*(1−2), 9–14.


Published on Web 09/28/2009

small metallic copper dendrites on the electrode surface.[30,31] Because the copper vanadium oxide powders retained much of their structural integrity with the formation of copper dendrites, it was proposed that copper vanadium oxides are well-suited for rechargeable systems because of the facility associated with copper insertion upon electrode oxidation (recharging).

Although not specifically stated in the copper vanadium oxide literature, we hypothesized that the formation of electrically conducting metal particles upon metal oxide reduction might result in an enhancement of electrical conductivity of the metal oxide, which should address conductivity problems for poorly conducting materials. Thus, we recently identified silver vanadium phosphorus oxide ($Ag_2VO_2PO_4$, SVOP) as a material of interest for next generation batteries, based on the desire to obtain the chemical stability observed in other phosphate cathode materials, achieve multiple electron transfer inherent in bimetallic materials, and provide the opportunity for the in situ generation of a conductive silver matrix.[32,33] In our initial communication, we reported that $Ag_2VO_2PO_4$ displays multiple electron transfer per formula unit with the associated high capacity as well as high current capability on discharge.[33]

With this report, we describe our approach to conductivity improvement via in situ silver metal formation, and thus rationalize the unexpected high current capabilities observed with $Ag_2VO_2PO_4$. Our strategy differs from prior methods of conductivity enhancement of metal oxides, as the $Ag_2VO_2PO_4$ conductivity is increased in situ with the initial reduction of the electroactive $Ag_2VO_2PO_4$ material. The electrochemical discharge process of $Li/Ag_2VO_2PO_4$ electrochemical cells is fully characterized, where structural and chemical changes in the $Ag_2VO_2PO_4$ cathode as a function of discharge are detailed, including formation of metallic silver nanoparticles and nanowires during discharge. To the best of our knowledge, this is the first study of this strategy applied to the $MPO_4$ class of materials, and while limited here to $Ag_2VO_2PO_4$, the concept should be applicable to families of metal oxides and phosphorus oxides which form conducting metal particles upon reduction.

## Experimental Section

**SVOP Synthesis.** The preparation of silver vanadium phosphorus oxide ($Ag_2VO_2PO_4$) via a topotactic exchange reaction of an organically templated vanadyl phosphate has been previously described.[34] A previously reported hydrothermal synthesis method was used to prepare $Ag_2VO_2PO_4$ for this study.[35] $Ag_2VO_2PO_4$ was produced on a 0.5 g scale by heating $Ag_2O$, $V_2O_5$, and $H_3PO_4$ in aqueous solution at 230 °C in a Teflon-lined autoclave for 96 h. The yellow powdered sample was collected using vacuum filtration and then dried under a vacuum.

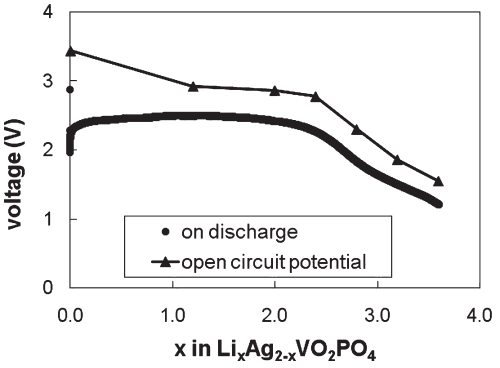


**Figure 1.** Constant current discharge of $Li/Ag_2VO_2PO_4$ cells.

**Physical Characterization.** X-ray diffraction (XRD) was measured using a Rigaku Ultima IV X-ray powder diffractometer, with Cu Kα radiation and Bragg−Brentano focusing geometry. Data were collected from 5 to 90° 2$\theta$ in continuous measurement mode, with a scan speed of 0.600°/min and a sampling width of 0.0200. Crystallite sizes were determined using the Scherrer equation after correcting for instrumental broadening using a $LaB_6$ standard.

Scanning electron microscopy (SEM) data was collected on a Hitachi SU-70 field emitting scanning electron microscope equipped with an Oxford Inca energy-dispersive X-ray spectroscopy (EDS) system. Secondary electron images were acquired at 5 kV. Backscatter electron images were observed and EDS data was collected at 20 kV.

**Cathode and Coin Cell Fabrication.** Coin cells were fabricated within an argon filled glovebox. Some cathodes were prepared containing pure, as synthesized $Ag_2VO_2PO_4$ material. For the pulsing study, $Ag_2VO_2PO_4$ was mixed with graphite and poly(tetrafluoroethane). Polypropylene separator material and 1 M $LiAsF_6$ in 50/50 (v/v) propylene carbonate/dimethoxyethane electrolyte were employed in all coin cells.

**Electrochemical Characterization.** For cells containing pure $Ag_2VO_2PO_4$ cathodes, AC impedance (ACI) measurements were performed using a CH Instruments model 604C Electrochemical Analyzer. Fresh coin cells were measured using the frequency range of 0.1 mHz to 100 kHz at 37 °C. Each coin cell was then discharged using a C/200 rate at 37 °C on a Maccor Series 4000 battery tester. Discharge was stopped at various depths of discharge (DODs) and cells were allowed to recover at open circuit potential until their rate of voltage change minimized. AC impedance was then measured at each DOD to a low frequency of 10 mHz. An amplitude of 5 mV was used for all ACI measurements. Analysis of the ACI data involved the instant fit approach where the segments of the initial semicircles of the data were fit to a basic equivalent circuit (Figure 8).

(26) Patridge, C. J.; Jaye, C.; Zhang, H.; Marschilok, A. C.; Fischer, D. A.; Takeuchi, E. S.; Banerjee, S. *Inorg. Chem.* **2009**, *48*, 3145–3152.
(27) Andrukaitis, E. *J. Power Sources* **1997**, *68*, 652–655.
(28) Li, H. X.; Jiao, L. F.; Yuan, H. T.; Zhao, M.; Zhang, M.; Wang, Y. M. *Mater. Lett.* **2007**, *61*, 101–104.
(29) Arico, A. S.; Bruce, P.; Scrosati, B.; Tarascon, J.-M.; Van Schalkwijk, W. *Nat. Mater.* **2005**, *4*, 366–377.
(30) Morcrette, M.; R, P.; Dupont, L.; Mugnier, E.; Sannier, L.; Galy, J.; Tarascon, J. M. *Nat. Mater.* **2003**, *2*(11), 755–761.
(31) Giorgetti, M.; Mukerjee, S.; Passerini, S.; McBreen, J.; Smyrl, W. H. *J. Electrochem. Soc.* **2001**, *148*(7), A768–A774.
(32) Iltchev, N.; Chen, Y. K.; Okada, S.; Yamaki, J. *J. Power Sources* **2003**, *119*, 749–754.
(33) Marschilok, A. C.; Takeuchi, K. J.; Takeuchi, E. S. *Electrochem. Solid-State Lett.* **2008**, *12*(1), A5–A9.
(34) Asnani, M.; Sharma, S.; Lofland, S. E.; Ramanujachary, K. V.; Buffat, P. A.; Ramanan, A. *Eur. J. Inorg. Chem.* **2005**, No. 2, 401–409.
(35) Kang, H. Y.; Wang, S. L.; Tsai, P. P.; Lii, K. H. *J. Chem. Soc., Dalton Trans.* **1993**, No. 10, 1525–8.

A three-electrode setup was used for slow scan rate voltammetry (SSRV). The working electrode was a platinum disk coated with a $Ag_2VO_2PO_4$:graphite mixture in the presence of poly(acrylic acid) . Lithium metal was used for the counter and pseudoreference electrodes. SSRV was performed inside an argon filled inert atmosphere glovebox, using electrolyte of 1 M $LiAsF_6$ in 50/50 (v/v) propylene carbonate/dimethoxyethane. A CH Instruments CHI604B potentiostat was used. Initial and final potentials of 3.5 V, and a lower potential of 1.5 V were used, with a scan rate of $2.00 \times 10^{-5}$ V/s.

For cells containing $Ag_2VO_2PO_4$ composite cathodes, each coin cell was discharged at 37 °C using a pulse discharge test on a Maccor Series 4000 battery tester. For the pulse discharge test, cells were discharged for five seconds at alternating high current densities of 10, 20, and 30 mA/cm$^2$, with low current discharge between pulses. The composite cathode data shown below (Figures 9 and 10) represent average values from three coin cells.

## Results and Discussion

The objective of this study was to investigate the changes in $Ag_2VO_2PO_4$ as it is reduced and lithiated during the discharge process in a primary lithium anode battery. As discussed below, metallic silver is a product of the $Ag_2VO_2PO_4$ reduction, so the lithiation process could be conceptualized as shown below (see reaction scheme 1). For simplicity, the general notation $Li_xAg_{2-x}VO_2PO_4$ is used when describing multiple levels of discharge. The notation $Li_yAg_{2-y}VO_2PO_4 + yAg^0$ is used specifically for $y < 2$, and the notation $Li_zVO_2PO_4 + 2Ag^0$ is used specifically for $z > 2$ to describe the reduced and lithiated material.

$$Ag_2VO_2PO_4 \xrightarrow{y\text{Li } (y<2)} Li_yAg_{2-y}VO_2PO_4 + yAg \xrightarrow{z\text{Li } (z>2)} Li_zVO_2PO_4 + 2Ag^0 \quad (1)$$

Samples of $Li_xAg_{2-x}VO_2PO_4$ where $x$ ranged from 0 to 3.6 were electrochemically generated. Specifically, the $Ag_2VO_2PO_4$ material was electrochemically reduced in a two electrode configuration using a lithium counter electrode and then isolated at various states of lithiation. The material samples were characterized to gain structural and compositional information about the discharge process as a function of lithiation.

The lithiation of $Ag_2VO_2PO_4$ was conducted at a current density of 0.32 mA/cm$^2$. As the cathodes reached the desired level of composition, discharge was halted and they were allowed to recover for several days at room temperature under zero current (Figure 1). The average initial open circuit voltage for the cells when first assembled was 3.44 V with a range of 3.41 to 3.46 V for the population of cells. The 24 h recovered open circuit voltage steadily decreased with discharge, where at a 90% discharge level the open circuit voltage reached 1.54 V. The electrochemically lithiated $Li_xAg_{2-x}VO_2PO_4$ samples were used for further analysis.

The $Li_xAg_{2-x}VO_2PO_4$ samples recovered from the discharged cells were used for analysis by scanning electron microscopy (SEM). Note the as-synthesized $Ag_2VO_2PO_4$ material has a uniform morphology, consisting of micrometer sized bladed particles (Figure 2). The individual particles are highly acicular, many with an aspect ratio $>20$. The images also show striations along the long axis of the particles indicating that many of the rods consist of assemblies of thinner planes of materials.

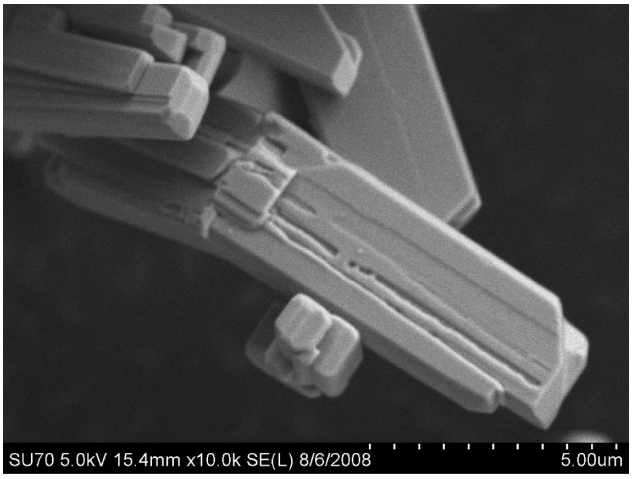


**Figure 2.** Scanning electron micrograph of $Ag_2VO_2PO_4$.

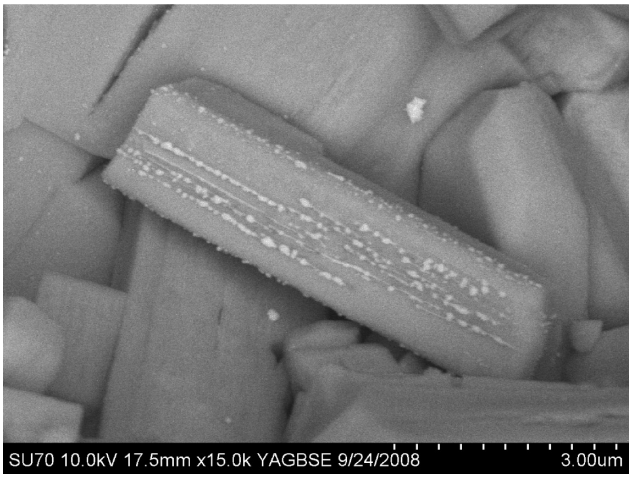


**Figure 3.** Scanning electron micrograph of $Li_{0.8}Ag_{1.2}VO_2PO_4 + 0.8Ag^0$.

SEM of the lithiated $Li_xAg_{2-x}VO_2PO_4$ material was collected at different levels of lithiation. A backscatter electron detector was used to provide atomic number contrast. Even at early states of lithiation, small bright nanoparticles were visible on the surface of the micrometer-sized bladed particles. A representative micrograph for $Li_{0.8}Ag_{1.2}VO_2PO_4 + 0.8Ag^0$ is shown (Figure 3). Nanoparticles appeared on the surface of the micrometer sized bladed particles, with a regular, layered arrangement where they were arranged along the long dimension of the particles.

The bright nanoparticles persisted at high depths of discharge for $Li_xAg_{2-x}VO_2PO_4$, and a smaller number of larger white particles were also observed. A representative micrograph for $Li_{1.6}Ag_{0.4}VO_2PO_4 + 1.6Ag^0$ is shown (Figure 4). Localized energy-dispersive X-ray spectroscopy (EDS) was collected at three locations of interest (Table 1). For locations A and C, the Ag:V:P ratio was

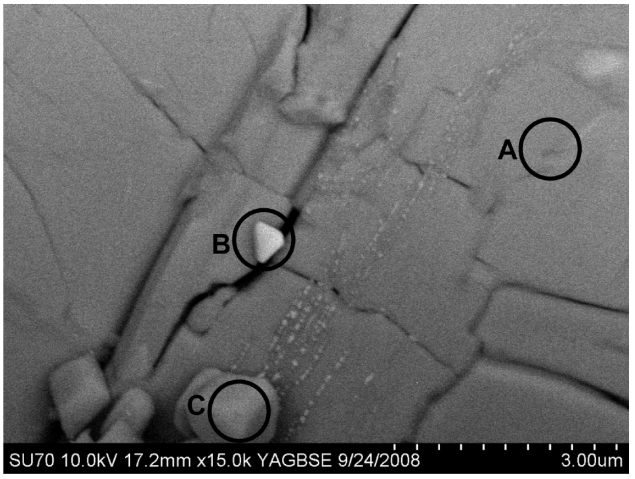


**Figure 4.** Scanning electron micrograph of $Li_{1.6}Ag_{0.4}VO_2PO_4 + 1.6Ag^0$.

**Table 1. Energy-Dispersive X-ray Spectroscopy of $Li_{1.6}Ag_{0.4}VO_2PO_4$ + $1.6Ag^0$**

| | atomic composition (%) | | |
|---|---|---|---|
| element | A | B | C |
| Ag | 25 | 32 | 17 |
| V | 13 | 7 | 8 |
| P | 14 | 10 | 11 |
| O | 48 | 52 | 64 |

approximately 2:1:1, consistent with an $Ag_2VO_2PO_4$ stoichiometry both on the flat surface and on the surface of the smaller gray micrometer sized particles. For the bright nanosized particle in location B, a higher Ag content was observed, consistent with our interpretation that the bright white regions are $Ag^0$ nanoparticles and nanowires formed on discharge.

X-ray powder diffraction (XRD) data were collected for the $Ag_2VO_2PO_4$ material as synthesized and for the lithiated material. A comparison of as synthesized material ($Ag_2VO_2PO_4$), a partially lithiated material ($Li_{1.2}Ag_{0.8}VO_2PO_4 + 1.2Ag^0$) and a highly lithiated material ($Li_{3.2}VO_2PO_4 + 2Ag^0$) is shown (Figure 5). The as-synthesized material showed excellent correlation to a literature pattern for $Ag_2VO_2PO_4$, with no extra peaks observed in our data.[36] As discharge progressed, the major $Ag_2VO_2PO_4$ peaks decreased in intensity or disappeared, and new peaks emerged. The newly formed peaks showed excellent correspondence to a literature file for silver metal (Figure 5). This observation is consistent with the formation of silver metal upon discharge of $Ag_2V_4O_{11}$.[37] To monitor changes as a function of discharge, the changes in the major $Ag_2VO_2PO_4$ peak (400) and the major Ag peak (111) intensity were plotted as a function of x in $Li_xAg_{2-x}VO_2PO_4$ (Figure 6). The $Ag_2VO_2PO_4$ peak intensity decreased linearly (open triangles in Figure 6) while the $Ag^o$ peak intensity increased linearly (open circles in Figure 6) up to $x = 2.4$. If the reduction mechanism of $Ag_2VO_2PO_4$ were to proceed stepwise with complete reduction of $Ag^+ \rightarrow Ag^0$, followed by reduction of $V^{5+}$, then the $Ag^0$ peak intensity would be expected to reach its maximum at $x = 2.0$. Therefore, this XRD data suggest that some reduction of $Ag^+$ and $V^{5+}$ occurs in parallel.

Crystallite size changes for $Ag^0$ were monitored. For crystallite size determination, the $Ag^0$ (220) and (311) peaks were selected. The $Ag^0$ crystallite size was small, and showed no systematic changes in either direction, with average sizes of $8.0 \pm 0.8$ nm in the (220) direction and $6.8 \pm 1.1$ nm in the (311) direction for $x = 2.0$ to 3.2 in $Li_xAg_{2-x}VO_2PO_4$, where the $\pm$ values represent two standard deviations.

Because the material analysis of the reduced $Ag_2VO_2PO_4$ confirmed the generation of silver nanoparticles, it was of interest to probe whether the nanoparticles had any functional impact on the resistance of the cathode material. Two-electrode cells were constructed with pure $Ag_2VO_2PO_4$ versus a lithium metal electrode. AC impedance was measured for the $Li/Ag_2VO_2PO_4$ cells as first assembled, and when they had been only lightly discharged to compositions of $x = 0.08$ and 0.2 in $Li_xAg_{2-x}VO_2PO_4$ (Figure 7). The Zview software package was used to determine the change in resistance of the cells with discharge. A simple equivalent circuit using a resistor, $R_s$, in series with two resistor/capacitor parallel combinations R1, C1 and R2, C2 was used (Figure 8). $R_s$, representing electrolyte and other ohmic resistance elements, stayed relatively constant at 6.3, 5.1, and 6.3 ohms for the three compositions measured. The resistance of the first semicircle, R1, also stayed fairly constant at 18, 22, and 19 ohms at $x = 0$, 0.08, and 0.2, respectively. However, there was a significant change in the resistance, R2, of the second parallel circuit element as the resistor value was 810 000 at $x = 0$ and decreased to 54.9 and 20.5 ohms at $x = 0.08$ and 0.2. This illustrates an increase in conductivity of $> 15\,000$ times as the cell was discharged from $x = 0$ to 0.08 or 2% of the cell theoretical capacity. The small change in R1, yet profound change in R2, is fully consistent with the significant increase in the $Li_xAg_{2-x}VO_2PO_4$ cathode conductivity early in the discharge of the cell. The change in R2 from $x = 0.08$ or 2% discharge to $x = 0.2$ or 5% discharge was much smaller as the resistance decreased by about a factor of 2 times. The significant decrease in resistance with initial discharge of the cells is consistent with the generation of a silver metal matrix within the cathode material as the $Ag_2VO_2PO_4$ cathodes are discharged with the reduction of $Ag^+$ to $Ag^0$ and the accompanying displacement of the silver from the vanadium phosphate structure.

The confirmation of silver metal as a discharge product and the significant increase in conductivity with only modest levels of lithiation provided incentive to further probe the electrochemical performance of $Ag_2VO_2PO_4$ as configured as a composite cathode versus a lithium metal anode. Two electrode coin cells were discharged using a pulse discharge test designed to test the ability of the $Ag_2VO_2PO_4$ material to deliver high pulse currents in a primary lithium battery. The cells delivered 215 mAh/g

(36) PDF no. 01−081−2149; valculated from FIZ#73580 3/18/08 by Jade.
(37) Leising, R. A.; Thiebolt, W. C.; Takeuchi, E. S. *Inorg. Chem.* **1994**, *33*(25), 5733–5740.

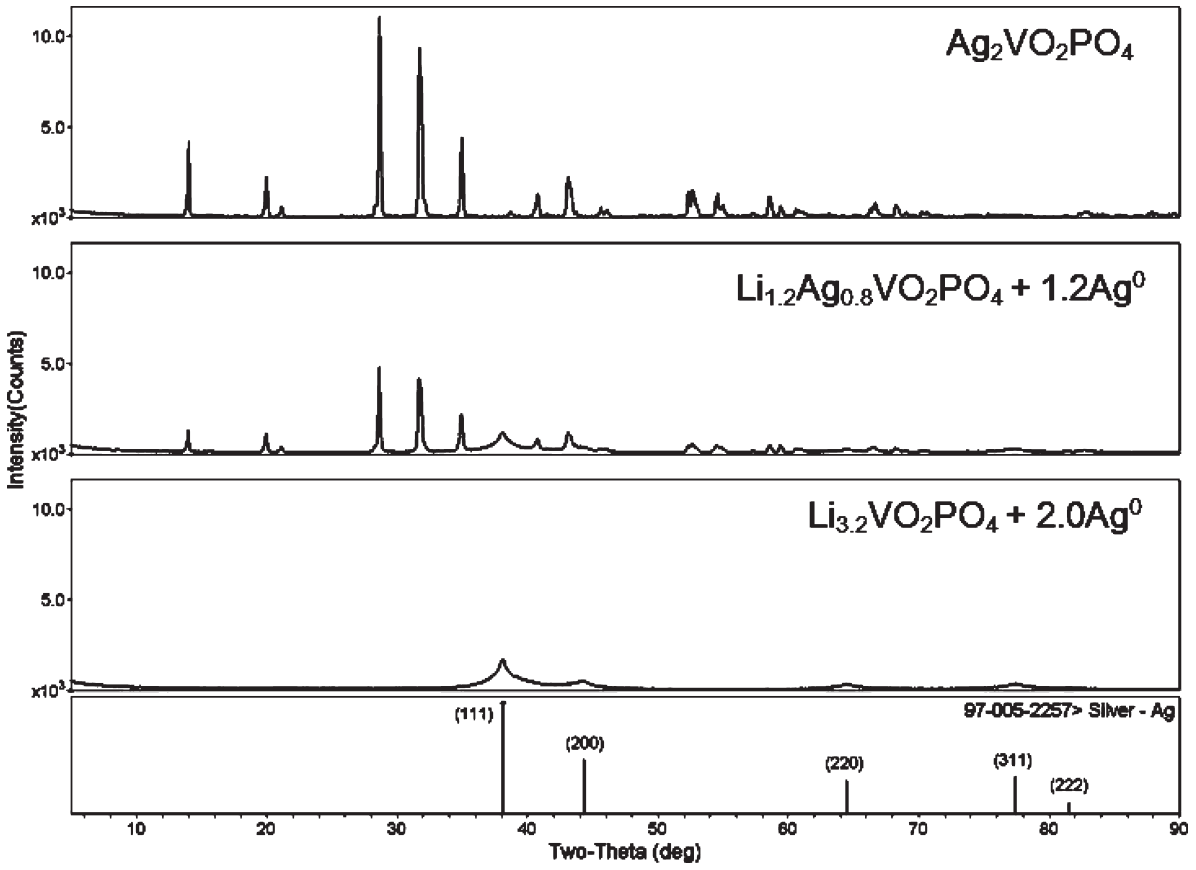


**Figure 5.** X-ray diffraction of $Ag_2VO_2PO_4$ and $Li_xAg_{2-x}VO_2PO_4$ ($x$ = 1.2, 3.2).

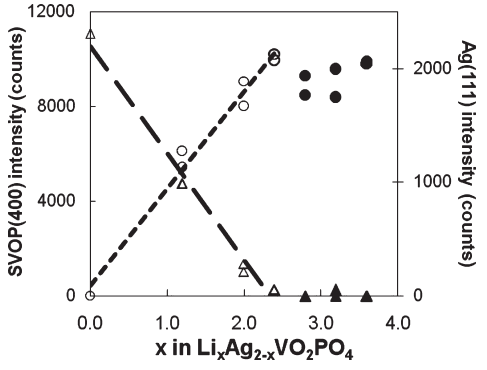


**Figure 6.** X-ray diffraction data analysis for $Li_xAg_{2-x}VO_2PO_4$ ($x$ = 0−3.6), $R^2$ for SVOP = 0.98, $R^2$ for Ag = 0.98.

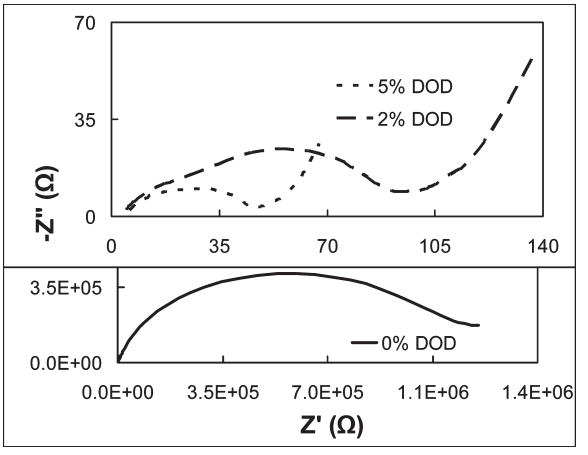


**Figure 7.** Impedance of $Li/Ag_2VO_2PO_4$ cells.

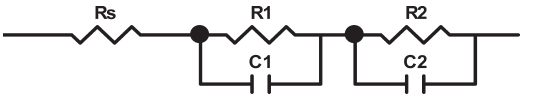


**Figure 8.** Equivalent circuit model used for $Li/Ag_2VO_2PO_4$ cells.

above 1.3 V pulse loaded voltage at 30 mA/cm$^2$ (Figure 9). We assigned the theoretical capacity as 272 mAh/g where it is assumed that reduction of $Ag^+$ to $Ag^0$ followed by reduction of the vanadium centers from $V^{5+}$ to $V^{4+}$ to $V^{3+}$ takes place. If reduction of $Ag^+$ to $Ag^0$ is followed by reduction of the vanadium from only $V^{5+}$ to $V^{4+}$, the theoretical capacity would be 204 mA h/g. Thus, based on a theoretical capacity of 272 mA h/g, ~80% of the $Ag_2VO_2PO_4$ material was accessed at the highest current density tested, yielding a material composition of $Li_{3.2}VO_2PO_4 + 2Ag^0$. The loaded voltage during the background segments of the discharge was fairly flat during the majority of discharge with some slope near the end of discharge.

The $Li/Ag_2VO_2PO_4$ battery resistance throughout cell life was calculated and assessed (Figure 10). Resistance was calculated using the difference between the prepulse voltage and the minimum voltage of the pulse, divided by the pulse current. Detailed examination of the RDC as a function of depth of discharge reveals a significant change as the cell discharge initiates. The calculated RDC during

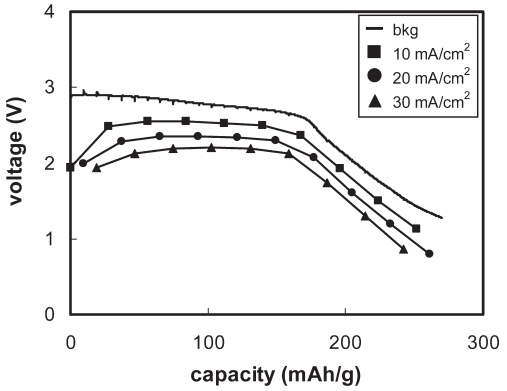


**Figure 9.** Background and pulse loaded voltages of Li anode/$Ag_2VO_2PO_4$ composite cathode cells.

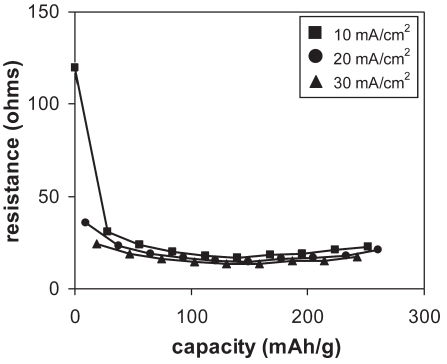


**Figure 10.** Resistance of Li anode/$Ag_2VO_2PO_4$ composite cathode cells.

the first applied pulse was 119 ohms. The second pulse applied at a current density of 20 mA/cm$^2$ or 3% DOD showed an RDC of 35 ohms and the third pulse under 30 mA/cm$^2$ or 7% DOD showed a value of 24 ohms. On return to a pulse current of 10 mA/cm$^2$ at 10% DOD, the RDC had decreased to 31 ohms, a factor of 3 reduction from its original value. This illustrates that the $Ag_2VO_2PO_4$ is initially more resistive, but rapidly becomes more conductive as discharge progresses consistent with the AC impedance results and the identification of silver metal as a discharge product. The decrease in resistance between the first and second pulse is most notable, indicating that only a small level of discharge is needed to significantly improve overall conductivity.

A three-electrode cell configuration was used to study the electrochemistry of the $Ag_2VO_2PO_4$ material when configured in a very thin layer on the surface of an electrode. Slow scan rate voltammetry data was collected for $Ag_2VO_2PO_4$ versus metallic lithium counter and pseudoreference electrodes (Figure 11). A major reduction

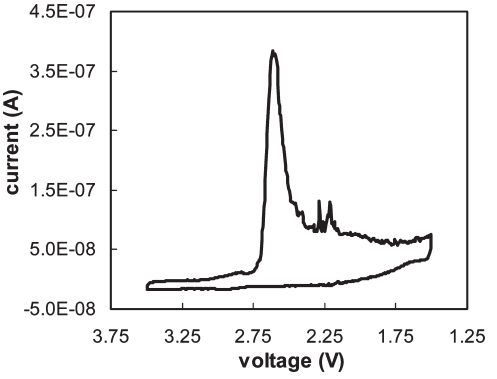


**Figure 11.** Slow scan rate voltammetry of $Ag_2VO_2PO_4$ versus Li.

peak was observed at 2.6 V, with a minor reduction peak at 2.9 V. These potentials are consistent with our previous observations of inflection points in an analysis of differential capacity versus voltage for the discharge of the Li/$Ag_2VO_2PO_4$ cell system.[33] Though not quantitative, the presence of one very large wave at 2.6 V in the voltammogram may indicate that under the three-electrode cell conditions, the reductions of silver and vanadium occur largely concurrently as was indicated by the XRD analysis. If the silver and vanadium reductions were significantly separated, we would expect reduction waves in a ratio of 2:1 for $Ag^+$ to $Ag^0$ reduction when compared with the reduction of $V^{5+}$ to $V^{4+}$ or $V^{4+}$ to $V^{3+}$.

## Conclusion

The reduction of silver vanadium phosphorus oxide ($Ag_2VO_2PO_4$) demonstrates the fundamental phenomenon that structural incorporation of a metal ion that is reduced to metallic particles or nanowires on initiation of reduction, leads to a significant increase in conductivity, in this case a factor of 15 000 times. This conductivity increase is of the material matrix itself independent of conductive additives. Additionally, silver vanadium phosphorus oxide can access four electrons per formula unit, resulting from the reduction of $Ag^+ \rightarrow Ag^0$ and $V^{5+} \rightarrow V^{4+} \rightarrow V^{3+}$. Conductivity increases achievable in bimetallic systems because of the formation of metallic nanowires or particles on reduction may be applicable not only to battery applications but also for other systems benefitting from inherent electronic conductivity.

**Acknowledgment.** This project was supported by the New York State Foundation for Science, Technology, and Innovation, the University at Buffalo (SUNY), and the National Institutes of Health under Grant 1R01HL093044-01A1 from the National Heart, Lung, and Blood Institute.